The Royal Society of Chemistry

Proofs for Correction

PCCP Production

Dear Author

Paper no. b315294d

Please check the proofs of your paper carefully. **Your proofs will not be read in detail by staff after you have returned them to us. It is your responsibility to ensure that the proofs have been read carefully**. Translation errors between word-processor files and typesetting systems can occur so the whole proof needs to be read even if an electronic file has been supplied. This proof reflects the content and general style of the paper without the stylistic complexity of the final printed page; however, the only differences should be minor layout changes such as different line breaks, tables being double column instead of single column and improvements in graphic placement. Please pay particular attention to: tabulated material (this may have been rekeyed); equations; numerical data; figures and graphics; and references. If you have not already done so and wish to indicate the corresponding author(s) please mark their name(s) with an asterisk.

We will endeavour to publish the article electronically on the RSC web site as soon as possible after we receive your corrections. **NB: No late corrections can be made hence please ensure that only your final corrections are notified to us**.

Please return your **final** corrections, where possible within 48 hours of receipt, to:

Mrs Sonya Spring, Serials Production, The Royal Society of Chemistry,
Thomas Graham House, Science Park, Milton Road, Cambridge, UK, CB4 0WF.
Tel: +44 (0)1223 432163; Fax: +44 (0)1223 432160; E-mail: proofs@rsc.org

Reprints—An electronic reprint file (in PDF format) will be supplied free of charge to the corresponding author. Free printed reprints are not provided. Enquiries about purchasing paper reprints should be sent to:

Miss Susan Bull, Production Operations Department (at the RSC Cambridge address given above).

Query reference	Query	Remarks
1.	The references have been renumbered so that they are cited in numerical order - please check.	

RESEARCH PAPER

PCCP
www.rsc.org/pccp

SIMS study of transition metal transport in single crystalline yttria stabilised zirconia†

Christos Argirusis,*[a] Marcela A. Taylor,‡[a] Martin Kilo,[a] Günter Borchardt,[a] François Jomard,[b] Bernard Lesage[c] and Odile Kaïtasov[d]

[a] *TU Clausthal, Institut für Metallurgie, Robert-Koch-Str. 42, D-38678 Clausthal-Zellerfeld, Germany. E-mail: christos.argirusis@tu-clausthal.de; Fax: +49 5323 723184; Tel: +49 5323 723189*

[b] *CNRS, Laboratoire de Physique des Solides et de Cristallogénèse, 1 Place Aristide Briand, F-92190 Meudon/Cedex, France*

[c] *L.E.M.H.E., Bât. 410, Université Paris-Sud, F-91405 Orsay Cedex, France*

[d] *C.S.N.S.M., Bât. 108, Université Paris-Sud, F-91405 Orsay Cedex, France*

Received 25th November 2003, Accepted 23rd April 2004
First published as an Advance Article on the web

The diffusion of Co, Fe and Ni in single crystalline yttria stabilized zirconia (YSZ) containing 9.5 mol% Y_2O_3 was studied in the temperature range between 1373 and 1673 K using secondary ion mass spectroscopy. Two different types of diffusion sources were used: thin oxide layers made by spin coating with a thickness of about 150 nm containing all three transition metals (Fe, Co and Ni) on YSZ single crystals and YSZ single crystals implanted with Ni (3×10^{16} ions cm^{-2}, 100 keV) at a mean depth of 45 nm. The determined diffusivities varied in the order $D(Fe) < D(Co) < D(Ni)$. Activation energies for the diffusion of the elements were determined to be 2.7 ± 0.4 eV, 3.9 ± 0.3 eV and 3.8 ± 0.3 eV for Fe, Co and Ni (3.6 ± 0.5 eV for implanted Ni), respectively. For the latter ion, the value of the activation energy was practically independent of the type of Ni source. The values for all elements were lower by 1–2 eV than for the host cation (Y and Zr) diffusion.

Introduction

The development of reliable devices based on ion conducting ceramics, such as solid oxide fuel cells (SOFC's) and gas sensors, has to take into account that these devices undergo a slight loss of performance over time. The degradation process is due to many processes; among them are interfacial reactions between the various components at the operating temperature of the devices or during their preparation. To achieve a better understanding of the fundamental degradation of a fuel cell, more has to be learned about the reactivity, transport and inter-diffusion properties of the various components of the devices.

For lower temperature operation, SOFC cathodes based on alternative materials other than doped $LaMnO_3$ are under consideration with complete or partial replacement of Mn at the B site in the perovskite structure by Co and/or Fe. These new electrode materials have much higher diffusion coefficients for oxygen ions and are electronically superior (faster kinetics of oxygen transfer at the electrode/electrolyte interface) compared to the conventional Sr or Ca doped $LaMnO_3$. However, these materials react at elevated temperatures even more vigorously with zirconia, where the reactivity increases in the order: $Mn < Fe < Co$ (see ref. 1 and references therein).

Up to now the most commonly used SOFC anode materials are Ni/zirconia cermets. The microstructure of the cermet plays a critical role in determining the performance and long-term stability of the anode. The most important reasons for anode degradation are attributed to the agglomeration of Ni particles, evaporation of Ni, and Ni dewetting of zirconia.[2]

Although some effort has been focused in the past few years on the study of the interaction between electrode and electrolyte in zirconia based SOFC devices,[3,4] only a little is known about the transport of transition metals in yttria stabilised zirconia (YSZ), except for some studies on Mn[5] and Fe[6,7] diffusion. The aim of the present study is to investigate the transport of Fe, Co and Ni in YSZ using secondary ion mass spectroscopy (SIMS).

Experimental

Single crystalline samples of YSZ containing 9.5 mol% Y_2O_3 polished on one side were provided by Crystal GmbH, Berlin.

Two kinds of diffusion sources were prepared:

- A benzene solution containing equal amounts of Fe, Co and Ni naphthenates was deposited on the polished surface of the polished single crystals by spin coating. The samples were heated up to 300 °C (2 K min^{-1}, 30 min) in order to burn out the organic residues. Thin films of about 150 nm thickness were obtained in this way.
- YSZ single crystals were also implanted with Ni of natural isotope composition (3×10^{16} ions cm^{-2}, 100 keV, starting from Ni metal) at a mean depth of 45 nm.

Diffusion anneals were carried out in air at 1100, 1200, 1300 and 1400 °C for 720, 96, 24 and 8 h, respectively, for the multiple cation diffusion. The annealing conditions for the Ni-implanted samples were 1100, 1200, 1300 and 1373 °C for 144, 72, 24 and 2.5 h, respectively.

SIMS experiments were performed using two different types of equipment: Cameca IMS 4f/5f with Cs^+ primary ion beam (10 keV, 30 nA) and Cameca IMS 3f with O^- primary ion

† Presented at the 85th Bunsen Colloquium on "Atomic Transport in Solids: Theory and Experiments", Gießen, Germany, October 31, 2003.

‡ On leave from University of La Plata, IFLP, CONICET Argentina, Member of Carrera del Investigador Científico CONICET Argentina.

DOI: 10.1039/b315294d

beam (10 keV, 120 nA), scanned over an area of 150×150 and 250×250 μm^2, respectively. Singly charged positive secondary ions (with O^- primary ion beam) and negative ions (Cs^+ primary ion beam) were detected. Charge compensation was performed using an electron flood gun. Furthermore, all samples were coated with a thin carbon layer. The depth of the crater, measured using a surface profiler (Tencor, Alpha-Step 500), was used to convert sputter time into depth. The depth inaccuracy resulting from the roughness of the crater bottom was no more than 10% in any case.

Diffusion profiles were determined by measuring the signal intensities of the isotopes, ^{54}Fe, ^{56}Fe, ^{59}Co, ^{60}Ni, ^{62}Ni, ^{89}Y, ^{90}Zr on sputtering. The signals of the diffusing elements were later normalised to the signal of zirconium in order to calculate the diffusion coefficients.

Bulk diffusivities D for the samples with a chemically deposited thin-film tracer source were calculated from the experimental results by fitting the following solution of Fick's second law for a thin film source of width $2h$ and concentration c_0 to the tracer isotope concentration profile:[8]

$$c(z, t) = \frac{c_0}{2}\left[\operatorname{erf}\frac{h-z}{2\sqrt{Dt}} + \operatorname{erf}\frac{h+z}{2\sqrt{Dt}}\right] \qquad (1)$$

Here c_0 is the concentration of the diffusant at $z < 0$ and $t = 0$, z is the depth coordinate and t is the diffusion time.

In the case of the implanted samples, the diffusion profiles were fitted using the equation[9]

$$\bar{c}(z, t) = \frac{Q}{\sqrt{2\pi\left(\Delta R_P^2 + 2Dt\right)}}\left\{\exp\left(-\frac{(z-R_P)^2}{2\Delta R_P^2 + 4Dt}\right) \pm \exp\left(-\frac{(z+R_P)^2}{2\Delta R_P^2 + 4Dt}\right)\right\} \qquad (2)$$

where Q is the implanted dose, R_P is the projected range and ΔR_P is the straggle determined from the as-implanted sample. In eqn. (2) the (+) sign is valid for the case of total reflection at the surface and the (−) sign is valid if the surface acts as a sink (for example due to evaporation of the diffusant). After integration of the depth profiles of the diffused samples we found that about 98% of the implanted dose disappeared to the surface from where it evaporated. Therefore the equation for a diffusing Gaussian implantation profile with a sink ((−) sign) was used.

Results and discussion

Fig. 1 shows the diffusion profiles of ^{59}Co, obtained at all the diffusion anneal temperatures. As can be seen, the mean penetration depth was in all cases more than 500 nm greater than the initial layer thickness. SEM/EDX analysis showed that even at the highest temperatures, the layer still remains. For calculating the diffusion coefficients, the parts of the profiles at penetration depths greater than about 150 nm were used.

Furthermore, it can be seen from the profiles that the interface between the layer and the zirconia substrate seems to be enriched with cobalt. This might indicate the formation of an interface layer, as reported *e.g.* for the formation of lanthanum zirconate, $La_2Zr_2O_7$, when annealing LSM/YSZ diffusion couples (LSM: $La_{1-x}Sr_xMnO_{3-\delta}$) form but it could also be an artefact (charging effect at the interface due to different conductivities in the layer and the substrate) during SIMS measurement. Since a similar behaviour was observed in the depth profiles of the other cations, it is more likely that it is a SIMS artefact at the interface between the tracer source and YSZ. At great penetration depths (beyond 1000 nm), transport along dislocations or sub-grain boundaries occurs, which is visible by the slowly decreasing tail in the diffusion profiles (Fig. 2). Therefore, for analysis of the bulk diffusion only, the region between 150 and 1000 nm can be used.

In Fig. 3, the profile determined in the as-implanted ^{60}Ni and the profile of the sample heated at 1100 °C for 144 h are represented for comparison. In the inset the local damage distribution (vacancies because of the implantation procedure) and the distribution of the implanted Ni ions as calculated with SRIM[10] are shown.

During the heat treatment, the Gaussian profile was depleted and significantly broadened compared to the as-implanted profile, and the diffusion coefficients were calculated using eqn. (2).

The diffusivities, obtained by fitting the data with eqn. (1) for the layer source and eqn. (2) for the implanted samples, were found to vary in the order $D(\mathrm{Fe}) < D(\mathrm{Co}) < D(\mathrm{Ni})$. It was shown in ref. 11 that the migration enthalpies are proportional to the charge densities of the cations as defined in eqn. (3).

$$\text{Charge density} = \frac{\text{charge}}{(\text{ionic radius})^3}\left[\mathrm{C\,\mathring{A}^{-3}}\right] \qquad (3)$$

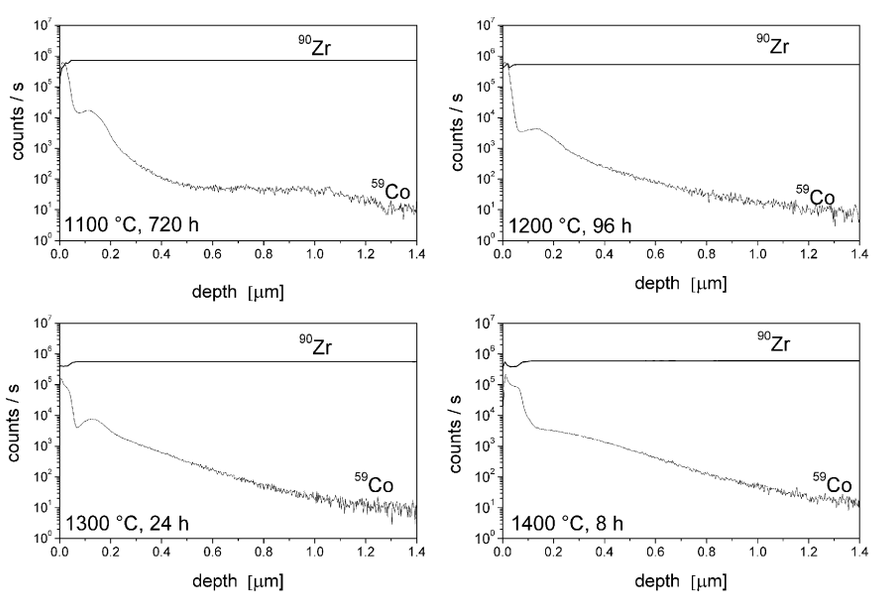

Fig. 1 Diffusion profiles for ^{59}Co isotope and ^{90}Zr matrix element.

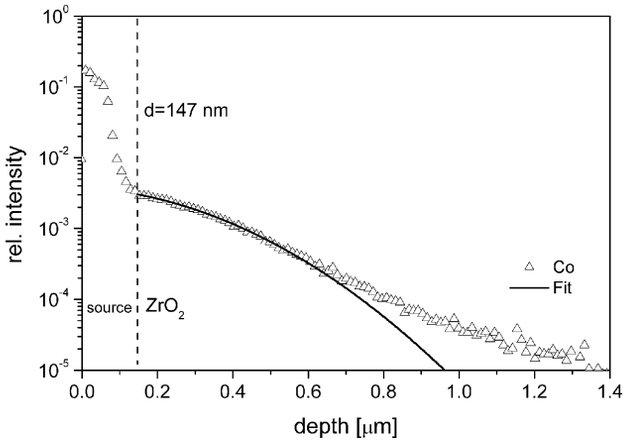

Fig. 2 Fitted ^{59}Co diffusion profile for a sample annealed at 1400 °C for 8 h.

Correspondingly, cation diffusion coefficients should be as high or as low as the charge density is. The charge densities for Fe^{3+} and Co^{2+} are 3.85 and 2.74 [C Å^{-3}] respectively; Ni^{2+} is not stable in the eightfold coordination.[12] Taking an estimated ion radius of 0.83 Å for eightfold coordination one gets a charge density of 3.5 [C Å^{-3}]. The order of the Fe^{3+} and Co^{2+} diffusivities corresponds to the respective charge density; for Ni^{2+}, we would expect its diffusivity close to that of Fe^{3+}, lower than that observed experimentally.

Fig. 4 represents the obtained diffusivities as a function of temperature for all samples investigated. From the Arrhenius plot, the activation energies for diffusion were determined to be 2.7 eV, 3.9 eV and 3.8 eV for Fe, Co and Ni, respectively.

In Table 1 diffusion coefficients, activation energies and preexponential factors for all the cations are summarized.

The obtained activation energies are for all the elements are about at least 1 eV lower than for the host cation diffusion (about 5 eV).[13]

Fe diffusion was investigated by de Ridder *et al.*[7] when studying the stability of Fe_2O_3 films on YSZ. The estimated diffusion coefficient for Fe at 800 °C was 10^{-19} cm^2 s^{-1}, one order of magnitude higher than the value obtained by extrapolation of the Arrhenius fit in the present study (2×10^{-20} cm^2 s^{-1}). Van Hassel *et al.*[6] obtained values for Fe diffusion of implanted samples of ceramic YSZ in the temperature range of 800–1400 °C which are two orders of magnitude higher than those reported by de Ridder *et al.*[7] and nearly three orders of magnitude higher than our values (see Fig. 4).

Comparing the diffusion coefficients obtained for Ni diffusion in the implanted and in the tracer-coated samples, the ones determined in the implanted sample are with respect to the error practically the same. As the activation energy is practically the same in both cases, the difference in the diffusivity could be due to the implantation-enhanced vacancy concentration. These vacancies are expected to relax quickly and therefore we measure an average diffusivity, which is slightly higher than the diffusivities measured with the tracer source. If the vacancies induced are partly the same as those involved in the cation diffusion mechanism in the experiments with a NiO tracer layer, then we do not expect a different activation enthalpy. Another explanation could be the crystal disorder induced by the implantation process. Diffusion coefficients in disordered solids are generally higher than in crystalline structures[6] and for YSZ, a very low equilibrium concentration of cation vacancies is estimated.[14] de Ridder *et al.*[7] have also attributed differences between diffusivities obtained from a layer source and an implanted source to crystal disorder produced by the implantation process on comparing their results with those obtained by Van Hassel *et al.*[6] in the case of Fe diffusion in YSZ.

Regarding the activation energy for Fe diffusion, the lower value for this ion compared to Ni and Co could be attributed to either a different valence of this metal as of Ni and Co or to a different pathway for the iron diffusion. On studying the stabilization of zirconia by iron addition Ghigna *et al.*[15] observed that the Fe ions at room temperature are mainly present in the oxidation state Fe(II) (together with a minor amount of 10% Fe(III)) when the products of the reaction

$$(1-x)\mathrm{Zr} + [(2-x)/3]\mathrm{Fe_2O_3} + \mathrm{O_2} \rightarrow \mathrm{Zr_{1-x}Fe_xO_2} + [(4-5x)/3]\mathrm{Fe} \quad (4)$$

(performed under 99.99% argon atmosphere) are rapidly quenched after the end of the combustion reaction. When the reaction product $Zr_{1-x}Fe_xO_2$ was allowed to cool down slowly to room temperature the average iron oxidation state was found to be between II and III. Contrary to that, in samples prepared by solid state reactions starting from cubic $(Zr,Y)O_2$ and Fe_2O_3, iron was found to be in the III oxidation state.[16] The authors also determined that the ions are located in

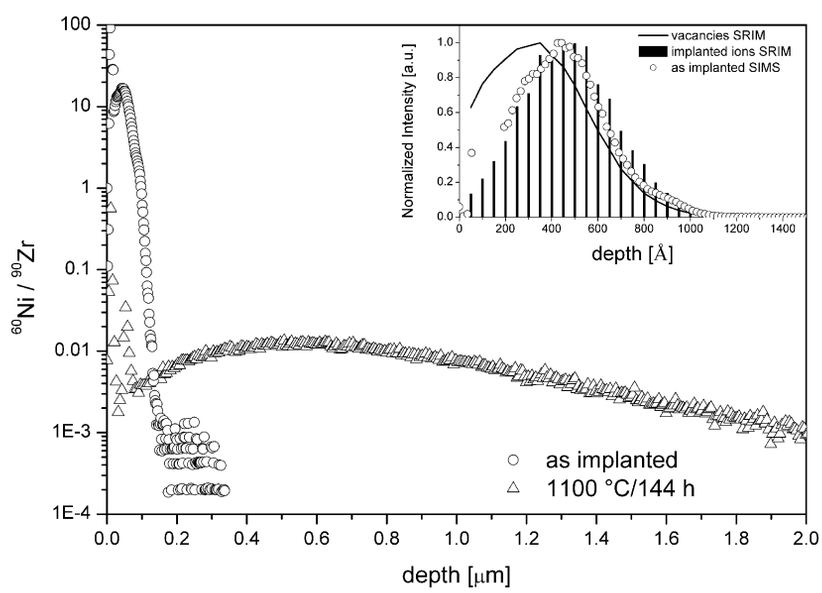

Fig. 3 Ni profile into YSZ for the as-implanted sample (○) and the sample heated at 1100 °C for 144 h (△). In the inset the implanted ion range (bar chart) and the defect concentration (solid line) caused by the implantation process are shown (SRIM calculation).

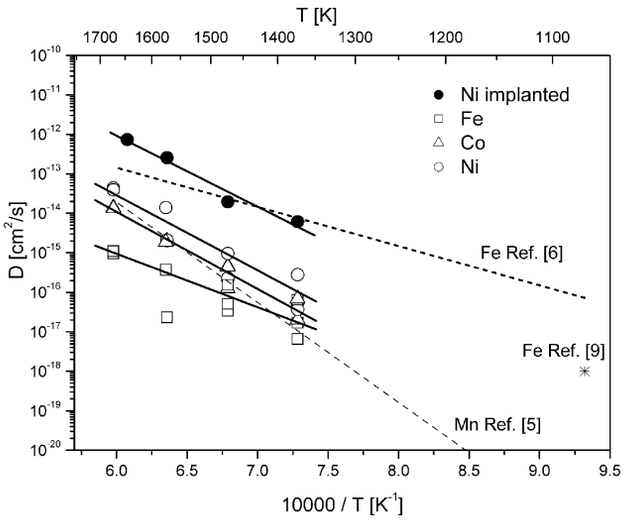

Fig. 4 Arrhenius plot of the diffusion coefficients. Symbols correspond to: ● implanted Ni, ○, △, □ deposited Ni, Co and Fe, respectively. The values obtained from refs. 5–7 are included for comparison.

Table 1 Summary of the experimental results

	D/cm^2 s^{-1}			
Temp/°C	Fe	Co	Ni	Implanted Ni
1100	6.6×10^{-18}	2.0×10^{-17}	3.7×10^{-17}	6.1×10^{-15}
	1.7×10^{-17}	6.9×10^{-17}	5.2×10^{-17}	
	6.5×10^{-17}		4.8×10^{-16}	
			2.8×10^{-16}	
1200	1.5×10^{-16}	4.4×10^{-16}	1.3×10^{-15}	6.9×10^{-14}
	5.1×10^{-17}	4.6×10^{-16}	3.6×10^{-16}	
	3.4×10^{-17}	1.3×10^{-16}	4.8×10^{-16}	
1300	4.4×10^{-16}	2.0×10^{-15}	2.0×10^{-15}	2.0×10^{-13}
		1.9×10^{-15}	2.1×10^{-15}	
			1.9×10^{-14}	
			1.4×10^{-14}	
1373				7.4×10^{-13}
1400	1.0×10^{-15}	1.4×10^{-14}	4.4×10^{-14}	
	9.6×10^{-16}	1.3×10^{-14}	3.9×10^{-14}	
	1.1×10^{-15}			
ΔH/eV	2.7 ± 0.4	3.9 ± 0.3	3.8 ± 0.3	3.6 ± 0.5
$\ln D_0$/cm^2 s^{-1}	-16 ± 3	-5 ± 3	-5 ± 4	-3 ± 3

roughly equal amounts at two different sites, a regular (0,0,0) zirconium site and the normally empty ($\frac{1}{2}$, $\frac{1}{2}$, $\frac{1}{2}$) site, giving rise to a 50/50 populated Fe'_{Zr} substitutional defect and a $Fe_i^{3\bullet}$ interstitial defect, which would be the first case for a cation to be in an interstitial position in zirconia. From EPR measurements Lajarvardi *et al.*[17] also found that in Fe-stabilized zirconia the Fe is present in the oxidation state 3+.

In order to elucidate the actual situation, further diffusion experiments under different atmospheres (different oxidation states of the diffusing cation) and molecular dynamics simulations (static lattice calculations using the program GULP[18] with previously published parameters[19]) to obtain migration energies of the diffusing cation in zirconia are planned. EXAFS analysis may be used to characterize short-range order and local structure in oxide solid solutions by direct measurement of the identity and number of next nearest neighbour (NNN) cations.[20]

Conclusions

SIMS experiments performed on the diffusion of Fe, Co, and Ni in YSZ allowed for the first time a comparison of the diffusion behaviour of these ions in YSZ. The diffusivities were found to increase as follows: $D(\mathrm{Fe}) < D(\mathrm{Co}) < D(\mathrm{Ni})$.

The activation energies for diffusion are 2.7 eV, 3.9 eV and 3.8 eV for Fe, Co and Ni, (3.6 eV for implanted Ni) respectively. They are about 1–2 eV lower than the activation energies for the host cation (Zr) and the stabilizer cation (Y), corresponding to slightly higher diffusivities of Fe, Co and Ni compared to the diffusivities of the host cations.

Acknowledgements

We acknowledge partial financial support of the Deutsche Forschungsgemeinschaft (DFG).

References

1 S. P. Badwal, *Solid State Ionics*, 2001, **143**, 39–46.
2 A. Khandkar and S. Elangovan, *Denki Kagaku Kogyo*, 1990, **58**, 551.
3 S. Faaland, M.-A. Einarsrud, K. Wiik and T. Grande, *J. Mater. Sci.*, 1999, **34**, 5811–5819.
4 K. Wiik, Ch. R. Schmidt, S. Faaland, S. Shamsili, M.-A. Einarsrud and T. Grande, *J. Am. Ceram. Soc.*, 1999, **82**, 721–728.
5 D. Waller, J. D. Sirman and J. A. Kilner, in *Proceedings of the Fifth International Symposium on Solid State Oxides Fuel Cells (SOFC V),Aachen, Germany, June, 2–5, 1997*, Electrochemical Society, NJ, 1997, vol. 97–18, pp. 1140–1149.
6 B. A. Van Hassel and A. J. Burggraf, *Appl. Phys. A: Mater. Sci. Process.*, 1991, **A53**, 155–163.
7 M. de Ridder, P. C. van de Ven, G. van Welzenis, H. H. Brongersma, S. Helfensteyn, C. Cremers, P. van der Voort, M. Baltes, M. Mathieu and E. F. Vansant, *J. Phys. Chem. B*, 2002, **106**, 13 146–13 153.
8 J. Crank, *The Mathematics of Diffusion*, Oxford University Press, Oxford, 1975, pp. 11–13.
9 H. Ryssel and I. Ruge, *Ion Implantation*, John Wiley and Sons, Chichester, UK, 1984.
10 J. Ziegler and J. Biersack, http://www.srim.org.
11 M. Kilo, R. A. Jackson and G. Borchardt, *Philos. Mag.*, 2003, **83**(29), 3309–3325.
12 R. D. Shannon, *Acta Crystallogr., Sect. A*, 1976, **32**, 751–767.
13 M. Kilo, M. A. Taylor, Ch. Argirusis, G. Borchardt, B. Lesage, S. Weber, S. Scherrer, M. Schroeder and M. Martin, *J. Appl. Phys.*, 2003, **94**, 7547–7552.
14 F. R. Chien and A. H. Heuer, *Philos. Mag. A*, 1996, **73**(3), 681–697.
15 P. Ghigna, G. Spinolo, U. Anselmi-Tamburini, F. Maglia, M. Dapiaggi, G. Spina and L. Cianchi, *J. Am. Chem. Soc.*, 1999, **121**, 301–307.
16 G. Spinolo, P. Gigna and U. Anselmi Tamburini, *ESRF Report, Experiment number CH372*, 20 August 1998.
17 M. Lajarvardi, D. J. Kenney and S. H. Lin, *J. Chin. Chem. Soc. (Taipei)*, 2000, **47**, 1065–1075.
18 J. Gale, *J. Chem. Soc., Faraday Trans.*, 1997, **93**(4), 629–637.
19 G. V. Lewis and C. R. A. Catlow, *J. Phys. C: Solid State Phys.*, 1985, **18**, 1149–1161.
20 G. A. Waychunas, W. A. Dollase and C. R. Ross, *Am. Mineral.*, 1994, **79**, 274–288.

